J. exp. Biol. **134**, 185–199 (1988)
Printed in Great Britain © *The Company of Biologists Limited 1988*

INDOOR FLIGHT EXPERIMENTS WITH TRAINED KESTRELS

II. THE EFFECT OF ADDED WEIGHT ON FLAPPING FLIGHT KINEMATICS

BY J. J. VIDELER, A. GROENEWEGEN, M. GNODDE AND G. VOSSEBELT

Department of Zoology, University of Groningen, PO Box 14, 9750 AA Haren, The Netherlands

Accepted 22 July 1987

SUMMARY

A male and a female kestrel were trained to fly over a mirror in a corridor, with lead weights attached to the feet to increase weight in the range 0–0·6 N (0–61 g). Films taken at 200 frames s^{-1} allowed three-dimensional analysis of the displacements of the head, tail and wingtips. A kinematic analysis, based on Fourier series, was made of the displacements in three perpendicular directions and of periodic changes of wing areas and tail areas.

With increased mass, there was a decrease in flight speed, increase in wing beat frequency, increase in vertical wing beat amplitude, and an increase in the inclination of the tail. The shorter wing beat cycle under load was mainly due to a decreased upstroke duration, implying that the relative importance of the downstroke was increased. The tail area and to a lesser extent the wing areas were enlarged during flights with the largest added weight.

INTRODUCTION

The preceding paper (Videler, Vossebelt, Gnodde & Groenewegen, 1988) demonstrated that kestrels (*Falco tinnunculus*) decrease their flight speed by 10% if their flight weight is increased by 30%. This implies that the induced power (proportional to the weight squared and inversely proportional to the span squared and to velocity) is almost twice as high. To discover how a kestrel achieves such an increase, it is necessary to study the flight mechanics of the animal under the different conditions. The unsteady character of flapping flight makes the use of a steady-state aerodynamic approach unrealistic. Rayner (1979*a*) taught us to concentrate on the vortex wake behind a bird in flapping flight, because it is the most important mechanism by which both lift and thrust are generated. The vortex wake

Key words: kestrel, kinematics, added weight effect.

approach requires knowledge of body mass, wing dimensions and wingstroke kinematic parameters. The wingstroke period, the duration of the downstroke and upstroke, the inclination of the stroke plane, the wing beat amplitude and the tilt angle of the body to the horizontal, describe the stroke geometry and are the key kinematic parameters in the vortex wake approach. Spedding (1987*b*) visualized the wake behind a kestrel in flapping flight, showing the relationship between the kinematic parameters, the shape of the vorticity distribution in the wake, and lift and thrust. Our objective was to detect changes in flight behaviour induced by added weight in terms of differences in key kinematic characteristics.

Brown (1948, 1953) studied wing beat kinematics of birds flying at different speeds, using a high-speed camera in fixed position in a closed corridor. He described the movements of various parts of the wings in great detail. We used a similar technique but concentrated the analysis mainly on periodic changes of a limited number of kinematic parameters. Fourier series are used to describe the periodic motion of the head, tailtip and wingtips in a three-dimensional frame of reference. Periodic changes of the areas of wing and tail and wingstroke and inclination angles were recorded during unloaded flights and flights with added weights up to one-third of the bird's body weight.

MATERIALS AND METHODS

Two wild adult kestrels, one female ('Kes') and one male ('Jowie') were trained to fly up and down between the gloves of two falconers in a 142 m long corridor at the Biological Centre in Haren. Short leather anklets, fitted around each leg, were replaced by lead ones, weighing either 0·3 N (mass 31 g) or 0·6 N per pair (61 g), during experiments with added weights. [See preceding paper (Videler *et al.* 1988) for further details.]

Cinematography

The movements during flapping flight of Jowie and Kes, with and without added weight, were filmed in side view and simultaneously from below with a Locam (Red Lake) 16 mm camera. This camera, with intermittent film transport and a timing LED (see Videler & Kamermans, 1985, for a detailed description), was mounted horizontally in fixed position in a side passage of the corridor. The optical axis of the lens was perpendicular to the longitudinal axis of the corridor. A 2·35 m long and 1·5 m wide mirror in the middle of the corridor, tilted at 45° to the horizontal plane, faced the camera. A bird flying along at about 1 m over the centre of the mirror appeared on the film in side and bottom views. We used indoor plants as obstacles to guide the birds over the centre of the mirror at the right height. Four filming lights of 850 W each provided enough light to film at 200 frames s^{-1} using Eastman Ektachrome 7250 film rated at 800 ASA. A reference grid in the ceiling over the mirror facilitated proper positioning of the camera. The camera was triggered with infrared-sensitive cells by the approaching bird, so that it was running at constant speed

before the bird entered the field of view. Slightly more than one complete flapping flight cycle could be recorded during each crossing.

The positions of the falconers with respect to the camera position made the birds cross the mirror at steady cruising speed.

Three-dimensional film analysis

Each frame of film contained a direct lateral image and a mirror image of the ventral side of the bird. The mirror image was treated as if it had been taken with another camera in the floor of the corridor. We adapted van Gheluwe's (1978) method to calculate two sets of coordinates for points appearing on both images in one three-dimensional frame of reference. The origin was the point where the camera's optical axis penetrated the mirror. The x-axis ran from the origin parallel to the longitudinal axis of the corridor. The vertical in the lateral image was the z-axis. The ventral image contained the origin, the x-axis and the horizontal y-axis, coinciding with the optical axis of the camera.

For each frame of a film sequence, both images of the beak, the tailbase and the point of the tail and the two wing tips were digitized with an HP 9874A digitizer and an HP 9835A computer. The surface areas of the projections on the horizontal plane of wings, body and tail were measured from the ventral image of each frame. Short film sequences of a three-dimensional reference grid, consisting of three perpendicular bars of known dimensions were analysed in the same way to determine the order of magnitude of the error of the method. Calculated dimensions along the y-axis were in one of the sequences on average 3·4 % longer than in reality, with a standard deviation of 3·3 %. The other calculated average dimensions along the x-, y- and z-axes always deviated less than 1·2 % from the real values and standard deviations were never larger than 4·5 %. Angles measured by our method were always within ±1·5 % of the real values.

Fourier analysis of cyclic events

Flapping flight is a cyclic motion where the time period T equals one complete up- and downstroke. Series of Fourier coefficients are most appropriate to describe cyclic events. We used the method of Videler & Hess (1984) to approximate T by fitting an harmonic function through the z-coordinates of the wing tips as a function of time.

Displacements in the x-, y- and z-direction of the beak, the tip of the tail and the wing tips are approximated with least square fitting methods by harmonic functions of the form:

$$f(t) = a_0 + b_0(t - t_c) + \sum_{j=1}^{3}\left(a_j \cos\frac{2j\pi t}{T} + b_j \sin\frac{2j\pi t}{T}\right), \quad (1)$$

where t_c is the time point of the central frame of the sequence, half-way between the first and last frame. The first two terms represent a straight line motion at constant speed, the others are Fourier terms describing the harmonic motion. a_0 is the average position and b_0 represents the average speed. We used three Fourier frequencies.

Higher terms were not included because those frequencies drown in the noise which was usually about ±8 mm. The amplitude of each Fourier frequency equals:

$$\sqrt{(a_j^2 + b_j^2)}. \tag{2}$$

Fig. 2 shows the actual displacements and the fitted functions in the x-, y- and z-directions of the beak, the tip of the tail and the wing tips.

The surface areas of the projections on the horizontal plane of tail and wings were also analysed as periodic functions with time period T. They are approximated by:

$$s(t) = a_0 + \sum_{j=1}^{3} \left(a_j \cos \frac{2j\pi t}{T} + b_j \sin \frac{2j\pi t}{T} \right). \tag{3}$$

The average surface area equals a_0 and the other terms describe the periodic changes as three sets of Fourier frequencies. (Higher frequencies are not included because their contributions remain within the limits of the measuring fault of ±4 cm^2.)

Kinematic parameters

We used the functions of the displacements of the beak in the x-direction to determine the average velocity V. The beak showed the smallest periodic motion in this direction and the velocities in the y- and z-direction were less than 3 % of the velocity in the x-direction. So V is estimated to equal b_0 of the displacement function along the x-axis.

During the upstroke the wing tip moves from the lowest to the highest position in the z-direction and back during the downstroke. We used the Newton–Raphson method to calculate the instants when the wing tip reached the highest (t_h) and the lowest (t_l) position along the z-axis and defined the durations of the up- and downstrokes (T_u and T_d) accordingly. The wing beat frequency is:

$$f = \frac{1}{T_u + T_d} = \frac{1}{T}. \tag{4}$$

The inclination of the stroke plane Φ was defined in the x–z frame of reference to be:

$$\Phi = \arctan \frac{\{W_z(t_h) - W_z(t_l)\} - \{B_z(t_h) - B_z(t_l)\}}{\{W_x(t_h) - W_x(t_l)\} - \{B_x(t_h) - B_x(t_l)\}}, \tag{5}$$

where $W_z(t)$, $W_x(t)$ and $B_z(t)$, $B_x(t)$ are displacement functions of the wing tip and beak along the z- and x-axes.

In the x–z frame of reference angles between the x-axis and the lines through beak and tail tip and tail tip and tail base represent the total angle of inclination (β) and the inclination of the tail (β_t), respectively. To obtain the angles of inclination relative to the flight direction, these angles were corrected for non-level flight by adding the angle δ between the flight path of the beak and the x-axis.

$$\delta = \arctan \frac{B_{0z}}{B_{0x}}, \tag{6}$$

where B_{0z} and B_{0x} are the beak velocities in the z- and x-directions.

RESULTS

Selection of sequences

The filming lights disturbed the birds at first, resulting in irregular wing movements over the mirror. They adapted quickly and we selected sequences without erratic wing movements of flights at uniform speed over the centre of the mirror. Results of detailed analyses of 13 sequences for Kes and seven for Jowie were used (Table 1). Six sequences for Kes (1–6) were without added weight, and the bird's mass was 198 g on average during these flights. Kes flew four sequences (7–10) with 31 g (0·3 N) and three (11–13) with 61 g (0·6 N) on her feet. The bird's average mass during sequences 7–13 was 190 g. Jowie weighed about 162 g during the seven sequences: flights 1 and 2 without added load, 3–5 with 31 g (0·3 N) and 6 and 7 with 61 g (0·6 N).

The exact frame rate was determined for each sequence to obtain the precise time between successive frames. The average frame rate was 198·2 (S.D. = 1·5) frames s^{-1}, providing on average 45 frames per sequence. Fig. 1 shows redrawn pictures of one wing beat of Jowie 1 and 7 (every fifth frame is drawn).

The fitting tightness

Digitized points and areas with their harmonic functions of Jowie 2 are drawn in Fig. 2 to give an impression of the closeness of the fit of our method. Fig. 2A–C shows the translations in the x-, y- and z-directions of the beak (*B*), tip of the tail (*T*) and wing tips (*LW* and *RW*) for every frame of the sequence. The left wing tip (*LW*) was away from the camera and disappeared behind the rest of the bird during parts of the sequence. Although the curves seem to fit reasonably well in this case, deviations were usually larger and functions of the wing tips away from the camera were not used in the analyses. We assumed symmetrical movements of the left and right wing. Fig. 2D gives measurements and functions of the horizontal projections of the total area of the bird (*BA*) and the area of body and tail (*TA*).

Table 1. *Average dimensions of one female (Kes) and one male (Jowie) kestrel during loaded and unloaded indoor flights*

Sequence no.	Body mass (kg)	Added mass (kg)	Total mass (kg)	Wing area (m^2)	(S.D.)	Wing loading ($N\,m^{-2}$)	Wingspan (m)	(S.D.)	Tail area (m^2)	(S.D.)
Kes										
1–6	0·198	0	0·198	0·0431	(0·0011)	45·13	0·48	(0·01)	0·0082	(0·0005)
7–10	0·189	0·031	0·220	0·0439	(0·0029)	49·01	0·47	(0·03)	0·0098	(0·0014)
11–13	0·189	0·061	0·250	0·0481	(0·0007)	51·01	0·49	(0·01)	0·0144	(0·0031)
Jowie										
1–2	0·162	0	0·162	0·0398	(0·0009)	40·02	0·48	(0·00)	0·0080	(0·0001)
3–5	0·162	0·031	0·193	0·0432	(0·0013)	44·14	0·52	(0·01)	0·0087	(0·0004)
6–7	0·162	0·061	0·223	0·0453	(0·0026)	48·07	0·55	(0·03)	0·0192	(0·0055)

Maximum span: Kes 0·72 m, Jowie 0·70 m.

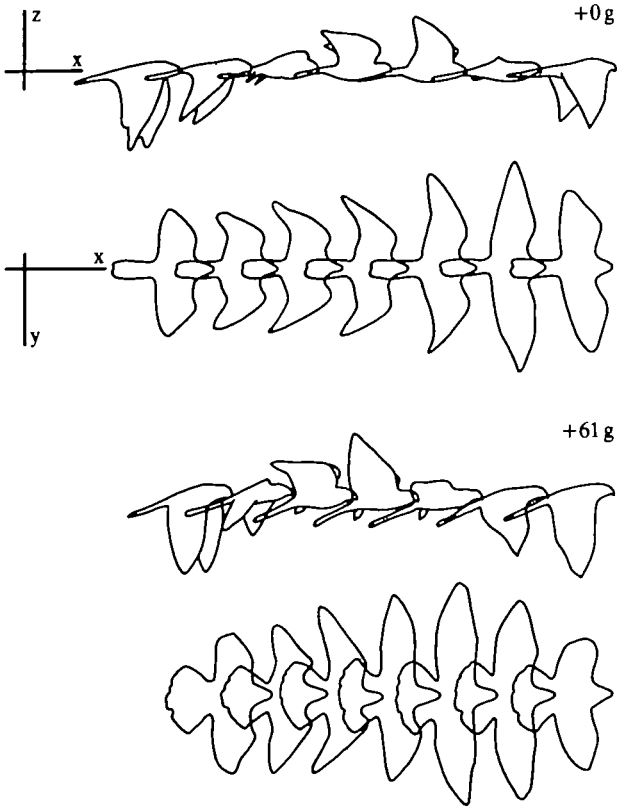

Fig. 1. Outlines of the lateral and the ventral view of a male kestrel at cruising speed without and with 61 g added load.

The root mean squares (RMS) of the deviations between digitized points and the harmonic equations give an impression of the tightness of the fit. The RMS of the beak displacements along the three axes varies between 1 and 3 mm and those of the point of the tail between 1–4 mm. The only exceptions are the displacements along the x-axis of beak and tail tip of Kes 3 with an average RMS of 5 mm. The deviations between the model and the displacements of the wing tips are slightly larger, with RMS varying between 2 and 6 mm and in two cases (Kes 11 and 13) up to 9 mm. The curves fitted to the areas are usually reasonably close with RMS within 5 % of the average values.

Description of a wing beat cycle

Fig. 3 exemplifies the harmonic functions during one period T of the displacement velocities and accelerations of the beak, tip of the tail and the right wing tip of Jowie 5. The velocity functions were obtained by differentiating the displacement functions (equation 1) and the accelerations by differentiating the velocity functions. The downstroke took 0·42 T and was shorter than the duration of the upstroke. The displacements in the x-direction were about 1·3 m in one period of 0·170 s accounting

for an average velocity of 7·7 m s^{-1}. Head and tail moved along straight lines in the x- and y-plots and showed oscillations of about ±1 cm around the average position in the z-direction. The wing tip moved away from the body during the beginning of the downstroke to a distance of 0·33 m from the body axis at 0·2 T and approached to 0·15 m at 0·6 T in the first part of the upstroke. The total excursion of the wing tip in the z-direction was about 0·35 m, and was slightly larger downwards from the average position than upwards. The velocity in the y-direction and accelerations in the x- and y-directions of beak and tail were zero on average. The small fluctuations were noise and had no physical meaning. Fluctuations of the velocities and accelerations of beak and tail tip were in counterphase, indicating small pendulations with period 0·5 T of the body axis in the x–z plane.

The wing tip velocity at the beginning of the downstroke reached a maximum value of about 10 m s^{-1}. During the first half of the downstroke and last part of the upstroke the wing tip velocity in the flight direction was greater than the average speed. The speed was lower during the rest of the period, with a minimum of 5 m s^{-1} at 0·6 T. The wing tip was pulled towards the body (y-direction) just before the end

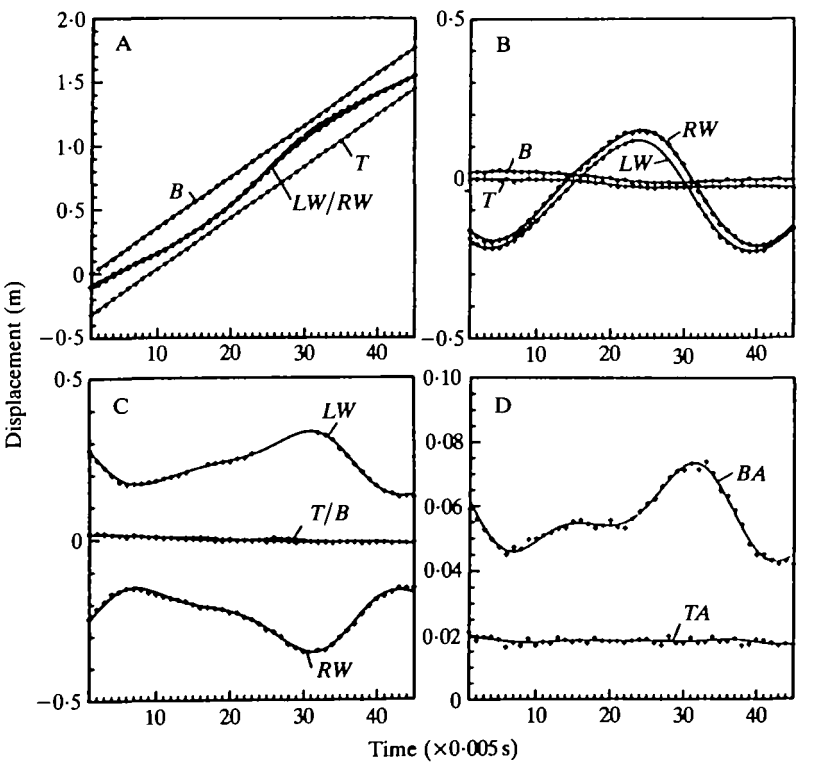

Fig. 2. (A–C) The position, digitized every 1/200 s, of the beak (*B*), the tip of the tail (*T*) and the wing tips (*LW*, *RW*) of a male kestrel flying indoors at cruising speed over a mirror. Digitized points and fitted functions in the x- (A), the z- (B) and the y- (C) directions are drawn. (D) The projections on the horizontal plane of the total surface area of the bird (*BA*) and of the tail area (*TA*), with their fitted functions.

of the downstroke at 5 m s^{-1} which was faster than the movement away from the body near the start of the downstroke, which reached 3 m s^{-1}. The maximum speed in the z-direction during the downstroke was 8 m s^{-1} and was faster than the upstroke maximum of 5·5 m s^{-1}. Wing tip accelerations in that direction reached two maxima of ±250 m s^{-2} during the downstroke. One was the downward acceleration at the beginning and the other the deceleration of the downward movement near the end.

The above description demonstrates the kind of kinematic information of the wingbeat cycle which is represented by the harmonic functions of the translations.

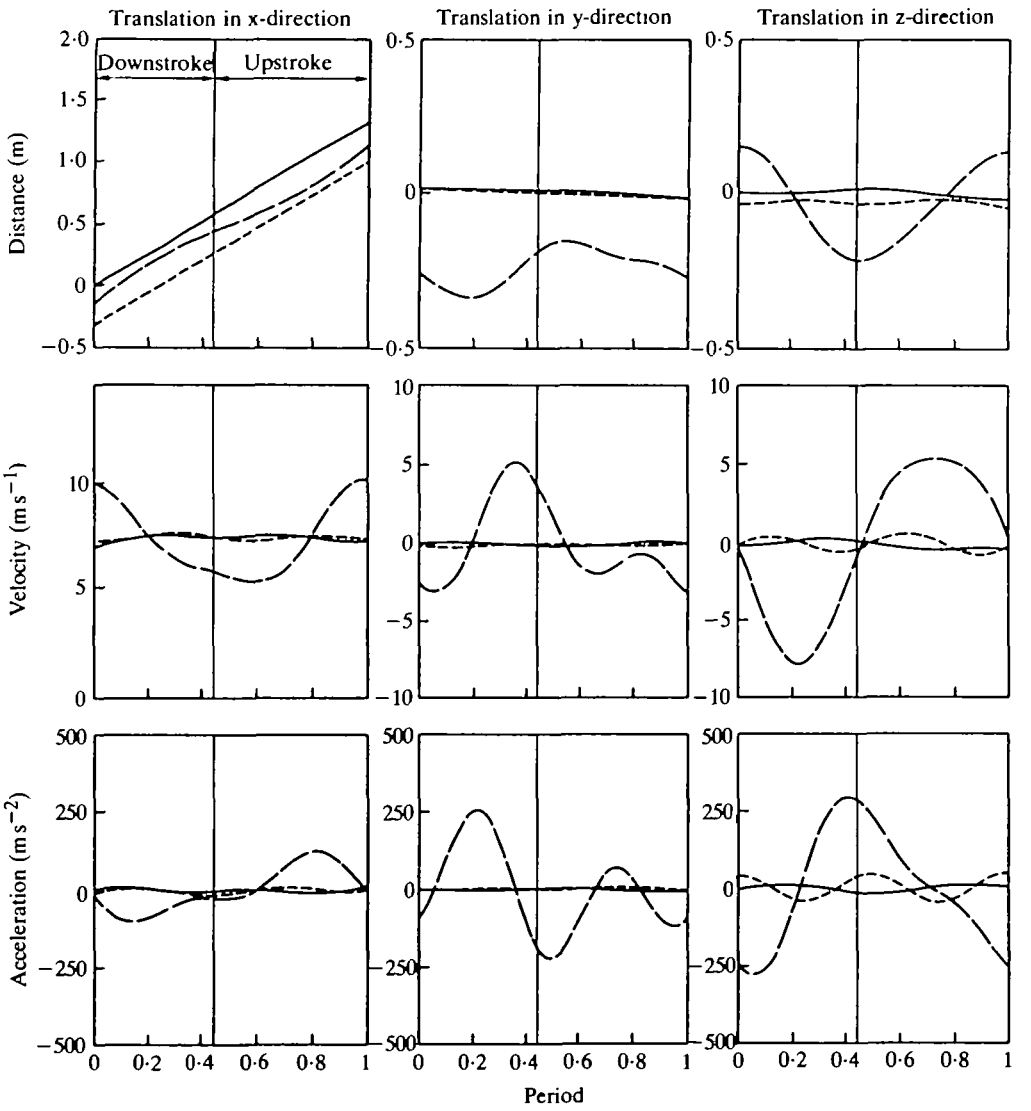

Fig. 3. The harmonic functions during one period T of the displacements, velocities and accelerations of the beak (solid line), the tip of the tail (dashed line) and the right wing tip (broken line) of a male kestrel carrying 31 g.

We will use these with the functions of the projected areas and the body and tail inclination angles to compare sequences of the two birds with and without added weight.

Displacements of the beak and tail tip

The contribution of the first Fourier frequency to the amplitudes of the harmonic functions is the only significant one here. The average amplitudes in the x- and y-directions of beak and tail tip of the two birds in our 20 sequences were smaller than 5 mm with standard deviations smaller than 3 mm. There were no obvious differences between the two birds, and added weight did not change the amplitudes in the x- and y-directions. The average amplitude in the z-direction of the beak was about 10 mm (S.D. = 2·3 mm) and similar in both birds during all flights. The average vertical movement of the tail tip was slightly over 8 mm and surprisingly smaller than that of the beak. Kes and Jowie showed the same range of figures, with the highest values during the 0·6 N added weight experiments.

Flight velocities were calculated from the beak functions in the x-direction and are included in Table 2. Jowie flew slower than Kes and his flight speed decreased with an increase of added weight, consistent with the results from the preceding paper (Videler *et al.* 1988). Kes flew 7·71 $m\,s^{-1}$ on average when loaded with 61 g and flew faster (8·13 $m\,s^{-1}$) unloaded. During the 0·3 N added-weight experiments, however, her speed was faster on average than during five out of six unloaded flights and reached 8·4 $m\,s^{-1}$.

Periodic wing motions

Wingbeat period, its frequency and the duration of upstroke and downstroke were determined from the wing tip functions and are given in Table 2. These data showed a frequency increase with increased weight. The velocity dropped despite shorter wingbeat periods. The main contribution to the shorter periods came from decreased upstroke durations. Fig. 4 indicates linear relationships between the upstroke duration and the period. The downstroke increase with larger periods is less obvious. Jowie's downstroke duration even showed a slight tendency to increase with the decrease of period. The relative importance of the downstroke increases in loaded flights as shown by the increased downstroke ratios.

The harmonic motions and the effect of added weight are illustrated in Figs 5 and 6. Fig. 5 compares the unloaded amplitudes in the three directions of Kes and Jowie. The amplitude patterns are very similar. The smaller excursion in the y-direction of Jowie was probably caused by the smaller span. Periodic changes of the movement amplitudes in the three directions under loaded conditions are shown in Fig. 6 for 0·6 N added weight. Main deviations from the zero load situations are the lower amplitudes in the x-direction and the higher amplitudes in the z-direction. The average figures of the amplitudes of the first Fourier frequency contributions showed these tendencies more quantitatively. The average amplitude in the x-direction of

Table 2. *Kinematic parameters of one female (Kes) and one male (Jowie) kestrel during loaded and unloaded indoor flights*

Sequence no.	Added weight (N)	Average velocity ($m s^{-1}$)	Wingbeat period, T (s)	Frequency, 1/T (Hz)	Upstroke duration, T_u (s)	Downstroke duration, T_d (s)	Downstroke ratio, T_d/T	Inclination angles total, β (degrees)	Inclination angles tail, β_t (degrees)	Wingstroke angle Φ (degrees)
Kes 1	0	8·69	0·185	5·41	0·105	0·080	0·43	4	14	91
2	0	8·05	0·182	5·50	0·102	0·080	0·44	3	14	88
3	0	8·15	0·176	5·68	0·099	0·077	0·44	3	15	93
4	0	7·64	0·173	5·78	0·102	0·071	0·41	4	16	91
5	0	8·10	0·182	5·50	0·100	0·082	0·45	2	11	88
6	0	8·12	0·191	5·24	0·111	0·080	0·42	4	14	94
Average	0	8·13	0·181	5·52	0·103	0·078	0·43	3	14	91
Kes 7	0·3	8·57	0·185	5·41	0·109	0·076	0·41	6	21	87
8	0·3	8·33	0·196	5·10	0·120	0·076	0·39	6	19	90
9	0·3	8·38	0·179	5·59	0·098	0·081	0·45	7	21	89
10	0·3	8·32	0·164	6·10	0·087	0·077	0·47	10	22	85
Average	0·3	8·40	0·181	5·52	0·104	0·077	0·43	7	21	87
Kes 11	0·6	7·66	0·160	6·25	0·085	0·075	0·47	9	22	91
12	0·6	7·80	0·161	6·21	0·087	0·074	0·46	7	21	92
13	0·6	7·68	0·164	6·10	0·089	0·075	0·46	10	23	89
Average	0·6	7·71	0·162	6·19	0·087	0·075	0·46	9	22	91
Jowie 1	0	8·10	0·163	6·14	0·095	0·068	0·42	3	13	85
2	0	8·02	0·179	5·59	0·100	0·079	0·44	4	11	87
Average	0	8·06	0·171	5·87	0·098	0·073	0·43	3	12	86
Jowie 3	0·3	7·83	0·163	6·14	0·090	0·073	0·45	6	18	85
4	0·3	7·88	0·177	5·65	0·099	0·078	0·44	9	20	83
5	0·3	7·74	0·170	5·88	0·094	0·076	0·45	6	20	86
Average	0·3	7·82	0·170	5·89	0·094	0·076	0·45	7	19	84
Jowie 6	0·6	6·81	0·153	6·54	0·078	0·075	0·49	12	26	78
7	0·6	7·46	0·168	5·95	0·091	0·077	0·46	11	20	82
Average	0·6	7·14	0·161	6·25	0·085	0·076	0·48	11	23	80

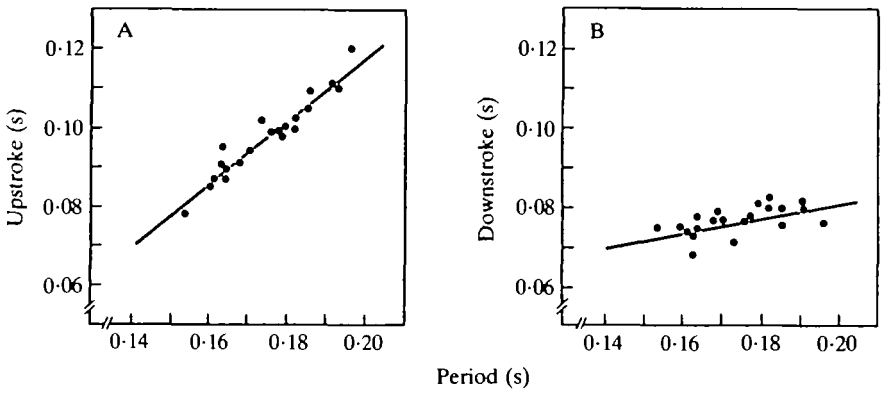

Fig. 4. Different upstroke and downstroke durations for different wingbeat periods during loaded and unloaded indoor flights of kestrels.

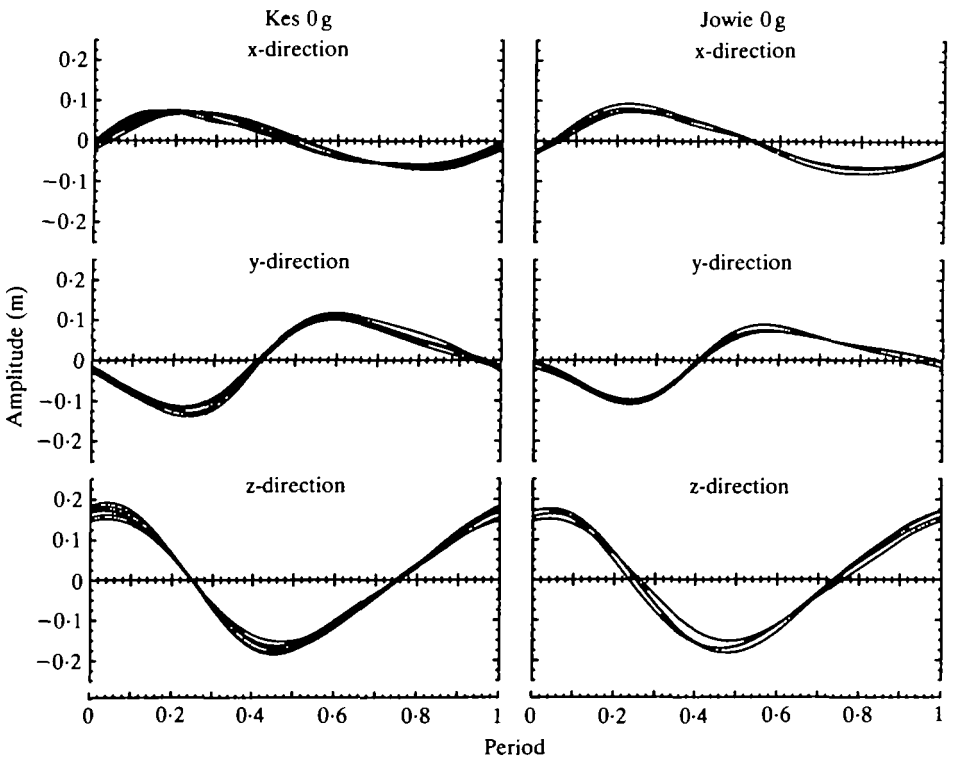

Fig. 5. The amplitudes of the harmonic motions of the wing tips over one period in the x-, y- and z-directions of a female and a male kestrel.

Kes carrying 61 g was 49 mm compared with 69 mm unloaded. In Jowie's case these figures were 59 mm compared with 78 mm. The average vertical wing tip displacements under 0·6 N added-weight conditions were 190 and 184 mm for Kes and Jowie,

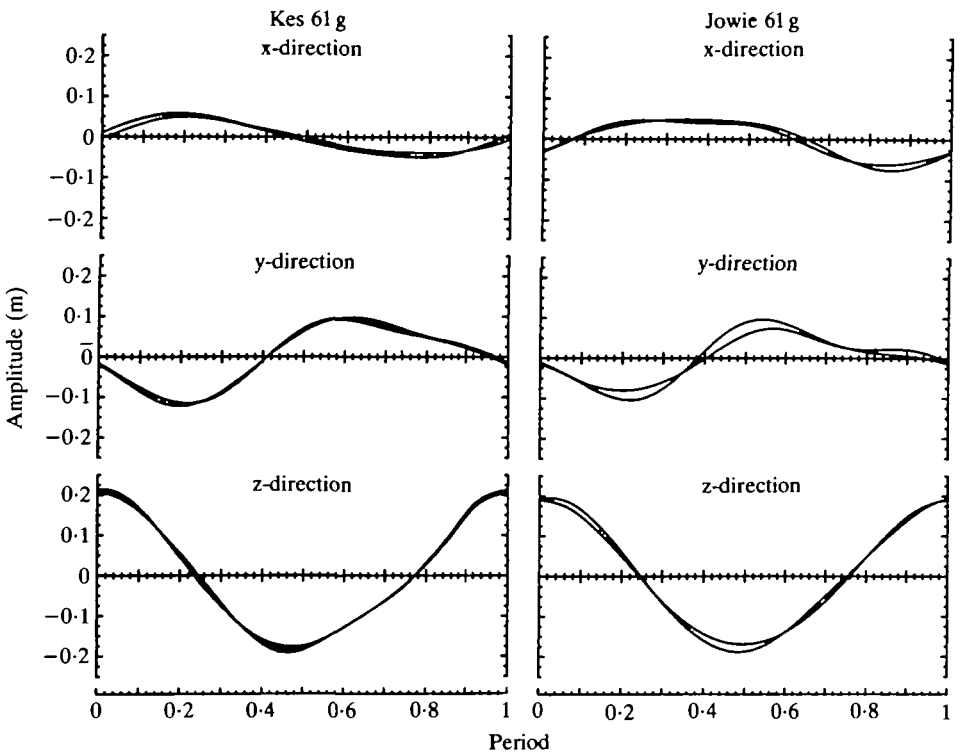

Fig. 6. The amplitudes of the harmonic motions of the wing tips over one period in the x-, y- and z-directions of a female and a male kestrel carrying 61 g of lead on their feet.

respectively. During unloaded flight these figures were 166 and 167 mm, respectively.

The wingstroke angles (Table 2) of Kes did not seem to be affected by increased weight. She beat her wings slightly more vertically than Jowie, whose wingstroke angles decreased by a few degrees with increased weight.

Wingspan and wing and tail areas

The maximum wingspan measured by stretching the wings manually without undue strain was 0·72 m for Kes and 0·70 m for Jowie. These values were never reached during flight. The average wingspan during the wingbeat cycles was between 60 and 80 % of the maximum values. The largest span occurred in the middle of the downstroke where it was 92 % of the maximum in the most extreme case (Jowie 6, Fig. 6, y-direction). The average wingspan values in Table 1 show a clear increase with increased weight for Jowie but not Kes. The cyclic changes around the average wingspan values did not seem to alter with increased weight (Figs 5, 6, y-directions).

The periodic changes of the wing area in ventral view were also not seriously affected by weight increase (Fig. 7). The average wing area, however, increased slightly with increased weight. The increase of the tail area was very marked (Fig. 1).

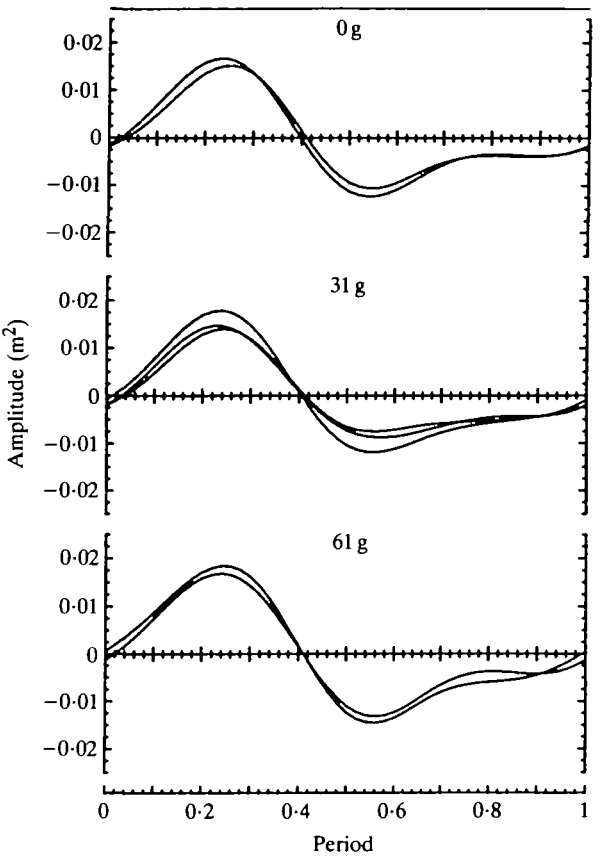

Fig. 7. Periodic deviations from the average wing area in ventral view of a male kestrel loaded with 0, 31 and 61 g.

The average values in Table 1 show a slight increase between 0 and 0·3 N added weight and very large average tail areas under 0·6 N load.

Angles of inclination

Table 2 shows that there is a slight increase in the total inclination and a large increase of the inclination of the tail. The bird probably uses its tail as a delta wing, with high angles of attack to create extra lift and consequently considerable drag (Hoerner & Borst, 1975), causing a decreased velocity with increased wingbeat frequencies. Unloaded, Jowie flew 1·38 m and Kes 1·47 m per wingbeat cycle. Carrying 61 g, Jowie covered only 1·15 m and Kes 1·25 m per period. The average frequencies increased from 5·87 and 5·52 Hz (Jowie and Kes 0 g) to 6·25 and 6·19 Hz (Jowie and Kes 61 g).

DISCUSSION

Delta wings are usually applied in supersonic aircraft and aerodynamic characteristics of triangular flat plates, collected by Hoerner & Borst (1975) for example, are

mostly derived from measurements aiming at the development of these aircraft. The parawing is a type of delta wing used at low speeds. These lifting planforms with a parachute-like tension structure are completely different from rigid delta wings. Hoerner & Borst (1975) showed that two-lobed parawings can have lift/drag ratios up to 10 for wings with an aspect ratio of 3. The aspect ratios during flights with the heaviest payload vary between 0·4 (Kes 13) and 2·5 (Jowie 6). The spread tail possibly acts as a multi-lobed parawing with tail feathers acting as keels. Flow visualization techniques (Spedding, Rayner & Pennycuick, 1984) and windtunnel tests are needed to unveil fully the aerodynamic effects of the spread-out tail.

There is no mention of the influence of the tail on the shape of the vortex trail in Spedding's (1987*a*,*b*) papers. His kestrel was obviously gliding and flapping with the tail closed and in line with the body as in our unloaded flights. The kinematic parameters of the kestrel crossing the helium bubbles in flapping flight (Spedding, 1987*b*) deviate substantially from our data. The average velocity of 7 m s^{-1} is about as low as for Jowie's 61 g flights, and the bird had about the same total body mass. The wingbeat period of 0·13 s was, however, much shorter and the downstroke ratio was larger than our data collected in Table 2. The body mass of Spedding's kestrel was 0·210 kg. This is the mass of a well-fed female and according to our experience slightly too high for optimal flight performance in captivity. There are, of course, further conceivable explanations for this discrepancy between the two studies. It is common knowledge among falconers (Glasier, 1982) that differences in flight performance between individuals of the same species and sex can be considerable. Important factors (apart from condition and weight) are training and history of the bird. Eyass birds (taken from the nest at an early stage), never fly as well as haggard birds that are taken from the wild as adults. Birds of prey kept in captivity for flight experiments must have their daily exercise to keep them in optimal flying condition. Indoor training requires many flights in a long corridor to exercise a bird properly (Kes flew up to 40 km in the corridor on a Sunday afternoon when persistent rain made training with the lure outside impossible).

Our experiments with kestrels in good flying condition show that weights attached to the feet had marked effects on the flapping flight kinematics. Flight speed decreased with increased mass, despite higher wingbeat frequencies and larger wingbeat amplitudes. These increased frequencies were mainly due to decreased upstroke durations. Tail area, wing area and the inclination of the tail increased under load.

It is a pleasure to thank Hanneke Videler for her falconry efforts. Dr D. Masman and many students helped to keep up the training schemes. Dr F. Hess advised on the three-dimensional and Fourier analyses. Financial support of the Hasselblad Foundation is gratefully acknowledged.

REFERENCES

BROWN, R. H. J. (1948). The flight of birds. *J. exp. Biol.* **25**, 322–333.

BROWN, R. H. J. (1953). The flight of birds. II. Wing function in relation to flight speed. *J. exp. Biol.* **30**, 90–103.

GLASIER, P. (1982). *Falconry and Hawking*. London: Batsford Ltd.

HOERNER, S. F. & BORST, H. V. (1975). *Fluid-Dynamic Lift*. Bricktown: Hoerner Fluid Dynamics.

RAYNER, J. M. V. (1979*a*). A vortex theory of animal flight. II. The forward flight of birds. *J. Fluid Mech.* **112**, 97–125.

RAYNER, J. M. V. (1979*b*). A new approach to animal flight mechanics. *J. exp. Biol.* **80**, 17–54.

SPEDDING, G. R. (1987*a*). The wake of a kestrel (*Falco tinnunculus*) in gliding flight. *J. exp. Biol.* **127**, 45–57.

SPEDDING, G. R. (1987*b*). The wake of a kestrel (*Falco tinnunculus*) in flapping flight. *J. exp. Biol.* **127**, 59–78.

SPEDDING, G. R., RAYNER, J. M. V. & PENNYCUICK, C. J. (1984). Momentum and energy in the wake of a pigeon (*Columbia livia*) in slow flight. *J. exp. Biol.* **111**, 81–102.

VAN GHELUWE, B. (1978). Computerized three dimensional cinematography for any arbitrary camera setup. *Biomechanics* **VI**, 343–348. Baltimore: University Park Press.

VIDELER, J. J. & HESS, F. (1984). Fast continuous swimming of two pelagic predators, saithe (*Pollachius virens*) and mackerel (*Scomber scombrus*): a kinematic analysis. *J. exp. Biol.* **109**, 209–228.

VIDELER, J. J. & KAMERMANS, P. (1985). Differences between upstroke and downstroke in swimming dolphins. *J. exp. Biol.* **119**, 265–274.

VIDELER, J. J., VOSSEBELT, G., GNODDE, M. & GROENEWEGEN, A. (1988). Indoor flight experiments with trained kestrels. I. Flight strategies in still air with and without added weight. *J. exp. Biol.* **134**, 173–183.